Formation of Interesting Organic Supramolecular Structures in the Solid-State Self-Assembly of Triphenol Adducts

ARTICLE *in* CRYSTAL GROWTH & DESIGN · SEPTEMBER 2005

Impact Factor: 4.89 · DOI: 10.1021/cg050251p

3 AUTHORS, INCLUDING:

Suresh Valiyaveettil
National University of Singapore
232 PUBLICATIONS **6,695** CITATIONS

CRYSTAL GROWTH & DESIGN
2006
VOL. 6, NO. 1
150−160

Formation of Interesting Organic Supramolecular Structures in the Solid-State Self-Assembly of Triphenol Adducts

Akhila Jayaraman, Venkataramanan Balasubramaniam, and Suresh Valiyaveettil*

Department of Chemistry, National University of Singapore, Singapore (S 117543)

Received June 3, 2005; Revised Manuscript Received August 1, 2005

ABSTRACT: Utilization of the interplay of dimensionality (1D, 2D, 3D), orientation of functional groups of the building blocks, influence of rigid/flexible linking groups, and weak interactions provides an interesting route for the creation of novel supramolecular architectures in the crystal lattice. Molecular complexes of triphenol **1** with aza compounds such as pyrazine (pyz), 1,10-phenanthroline (phen), 4,4′-bipyridyl (bpy), *trans*-1,2-bis(4-pyridyl)ethylene (bpy-ethe), and 1,2-bis(4-pyridyl)ethane (bpy-etha) have been investigated using X-ray diffraction techniques. The rigid 3D triphenol **1** self-assembles to form a distorted ladder, which organizes into columns via O−H···O hydrogen bonds. Self-assembly of complexes **1·pyz** and **1·bpy-ethe** result in ladder-type structures with pyz and bpy-ethe molecules forming the rungs of the ladder. The molecular components in complex **1·phen** aggregate into 1D hydrogen-bonded chains. A 4-fold self-clathration was observed in the crystal lattice of **1·bpy**. Owing to the expanded lattice of the complex **1·bpy-etha**, one of the reactant molecules of bpy-etha fills the spaces as guest molecules. The nature of the aza groups helps to enhance the overall volume of the crystal lattice thus leading to the formation of various supramolecular assemblies.

Introduction

Successful crystal engineering strategies involve manipulation of noncovalent interactions such as hydrogen bonding between complementary molecular aggregates to control their self-assembly in the solid state.[1] The ability of the H-bonds to distinguish among recognition patterns has been exploited for the noncovalent synthesis of interesting supramolecular architectures.[2] It is now established that weak hydrogen bonds associated with the aromatic system play an important role in the molecular recognition process.[3]

Phenol−aza/amine interactions provide a predictable and robust organizing force that has been exploited for the rational design of new materials[4] and template-assisted synthetic strategies.[5] The specificity of O−H···N bonds involved in the molecular complexes has been utilized for the generation of a variety of supramolecular aggregates.[6−8]

Molecules with C_3 symmetry represent useful materials for studies relating to host−guest complexation and nonlinear optics.[1b,9] Recently, the solid-state self-assembly of polyphenols that possess C_3 symmetry has been reported in detail by us.[10] The purpose of the study was to design and synthesize a series of related compounds whose chemical structure could be modified systematically to utilize the strength and directionality of the hydroxyl groups to generate interesting supramolecular structures. Based on the above rationale, the supramolecular organization in 3D triphenols, tetraphenol, and pentaphenol was investigated.[10] The triphenols having hydroxyl groups meta and para to the tertiary carbon atom self-assemble into helical and ladder-type architectures. In this paper, the crystal structure of another related triphenol (**1**) is reported. Two hydroxyl groups on adjacent phenyl rings are oriented ortho to the tertiary carbon, while the hydroxyl group on the third phenyl ring is para substituted. Also, the versatility of triphenol **1** to establish complementary interactions with diamines has been explored to derive supramolecular adducts with aza compounds such as pyrazine (pyz), 1,10-phenanthroline (phen), 4,4′-bipyridine (bpy), *trans*-1,2-bis(4-pyridyl)ethylene (bpy-ethe), and 1,2-bis-(4-pyridyl)ethane (bpy-etha) (Figure 1). It is anticipated that the interplay of competing hydrogen-bonded interactions (e.g., O−H···N and O−H···O), rigidity of the 3D triphenol, and flexibility of the added bases would control the molecular organization in the crystal lattice to yield various supramolecular architectures.

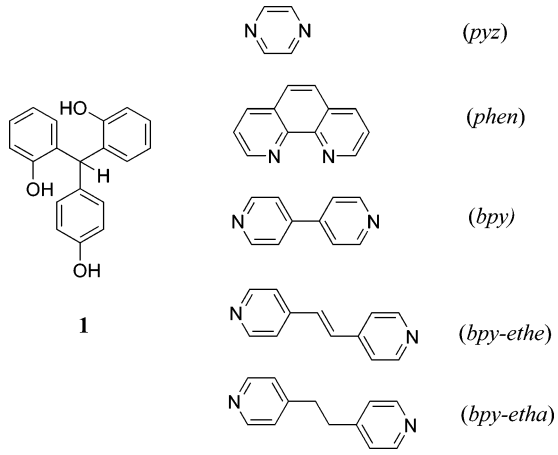

Figure 1. Molecular structure of triphenol (**1**) and the aza compounds.

Experimental Section

General. All reagents were used as received without further purification unless stated otherwise. Tetrahydrofuran (THF) was distilled over sodium under N_2 atmosphere. Pyrazine (pyz), 1,10-phenanthroline (phen), 4,4′-bipyridine (bpy), *trans*-1,2-bis(4-pyridyl)ethylene (bpy-ethe), 1,2-bis(4-pyridyl)ethane (bpy-etha), 2-bromophenol, benzyl bromide, anhydrous potassium carbonate, ethyl-4-hydroxybenzoate, and 1-butanone were purchased from commercial sources. Magnesium turnings (Grignard grade) were precleaned, dried in the vacuum oven at 105 °C, and cooled under argon atmosphere. Silica gel 60 F_{254} plastic-backed plates (20 cm × 20 cm) were used for thin-layer chromatography (TLC). Column chromatography was carried out using silica gel 60 (230−400 mesh). The ^{1}H and ^{13}C NMR spectra were recorded on Bruker ACF-300 spectrophotometer with trimethylsilane (TMS) as the internal standard. All melting points were determined with a Reichert−Jung Thermo Galen hot stage microscope and uncorrected. FT-IR spectra were recorded on a Perkin-Elmer 1710 infrared Fourier transform spectrometer. Mass spectra (MS-ESI) were determined using a Finnigan MAT LCQ or Finnigan TSQ 7000 mass spectrometer at an

* E-mail: chmsv@nus.edu.sg.

10.1021/cg050251p CCC: $33.50
Published on Web 09/27/2005

Scheme 1[a]

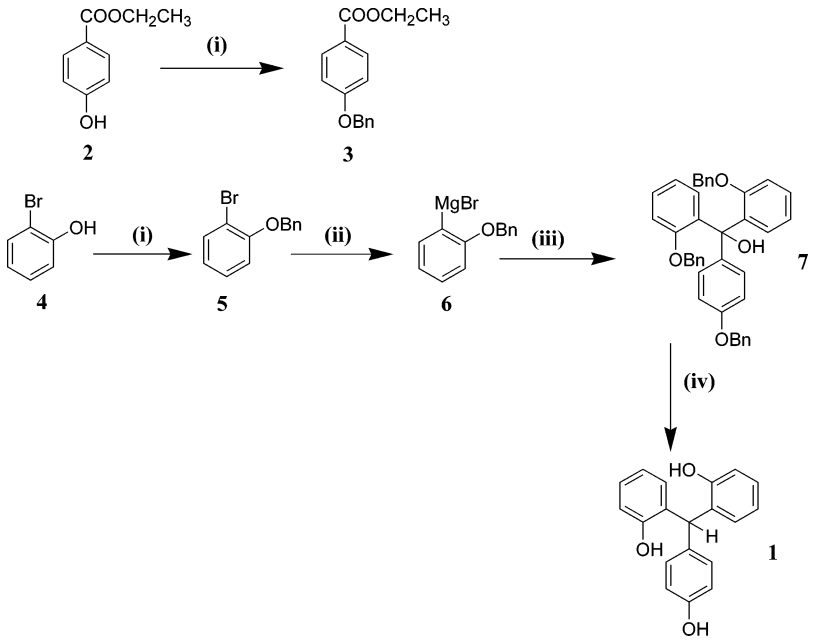

[a] Reagents: (i) benzyl bromide, K_2CO_3, 1-butanone, 80 °C; (ii) Mg, I_2, 0 °C−rt; (iii) **3**, 0 °C−rt, NH_4Cl; (iv) $Pd(OH)_2/C$, H_2, 2−3 mbar, $CH_3OH/THF/H_2O$ (1:1:0.1).

Table 1. Selected Crystal Data and Structural Refinements of Triphenol 1 and Its Adducts

	1	**1·pyz**	**1·phen**	**1·bpy**	**1·bpy-ethe**	**1·bpy-etha**
empirical formula	$C_{19}H_{16}O_3$	$C_{19}H_{16}O_3 \cdot (C_4H_4N_2)_{0.5}$	$C_{19}H_{16}O_3 \cdot (C_{12}H_8N_2)_2 \cdot C_4H_8O \cdot (O_2)_{0.5}$	$C_{19}H_{16}O_3 \cdot (C_{10}H_8N_2)_{1.5}$	$C_{19}H_{16}O_3 \cdot (C_{12}H_{10}N_2)_{0.5} \cdot H_2O$	$C_{19}H_{16}O_3 \cdot (C_{12}H_{12}N_2)_2$
formula weight	292.32	332.36	733.84	526.59	784.87	660.79
crystal system	orthorhombic	triclinic	triclinic	monoclinic	triclinic	triclinic
space group	*Pbca*	$P\bar{1}$	$P\bar{1}$	$P2_1/c$	$P\bar{1}$	$P\bar{1}$
a, Å	15.189(2)	8.263(1)	11.305(3)	7.395(7)	9.1353(5)	11.353(7)
b, Å	7.500(9)	10.042(2)	12.491(3)	18.419(2)	10.447(6)	12.323(7)
c, Å	25.839(3)	10.373(2)	14.381(4)	20.333(2)	12.097(7)	13.698(8)
α, deg	90	90.401(3)	100.202(6)	90	106.018(1)	107.633(1)
β, deg	90	102.338(3)	95.766(5)	90.785(2)	105.787(1)	102.933(1)
γ, deg	90	96.760(4)	103.474(6)	90	97.434(1)	93.574(2)
Z	8	2	1	4	1	2
V, Å^3	2943.6 (6)	834.4(2)	1922.2(9)	2769.4(5)	1041.42 (10)	1762.7(2)
D_{calc}, g cm^{-3}	1.319	1.323	1.266	1.263	1.251	1.245
absorption coefficient, mm^{-1}	0.089	0.089	0.082	0.082	0.083	0.079
F(000)	1232	350	772	1108	414	700
crystal size, mm^3	0.50 × 0.34 × 0.30	0.50 × 0.40 × 0.26	0.40 × 0.38 × 0.04	0.40 × 0.36 × 0.30	0.30 × 0.24 × 0.10	0.50 × 0.20 × 0.16
index ranges	$-16 \le h \le 18$ $-8 \le k \le 8$ $-28 \le l \le 30$	$-6 \le h \le 10$ $-13 \le k \le 11$ $-13 \le l \le 13$	$-14 \le h \le 14$ $-16 \le k \le 16$ $-18 \le l \le 18$	$-9 \le h \le 9$ $-23 \le k \le 18$ $-25 \le l \le 26$	$-10 \le h \le 10$ $-12 \le k \le 12$ $-14 \le l \le 14$	$-14 \le h \le 14$ $-16 \le k \le 16$ $-17 \le l \le 17$
R(int)	0.1026	0.0190	0.0538	0.0349	0.0224	0.0401
max/min transmission	0.9739/0.9570	0.9773/0.9570	0.9967/0.9678	0.9759/0.9681	0.9917/0.9754	0.9875/0.9616
data/restraints/params	2586/0/211	3770/0/238	8825/0/517	6360/0/373	3671/3/280	8079/0/463
R_1	0.0815	0.0433	0.0593	0.0616	0.0605	0.0607
wR_2	0.1619	0.1165	0.1339	0.1317	0.1565	0.1232
GOF	1.134	1.080	0.977	1.026	1.027	1.038
θ range, deg	1.58−25.0	2.04−27.46	1.71−27.50	1.49−27.49	1.85−25.0	1.61−27.50
reflns collected	15587	5840	25270	19306	10922	23198
independent reflns	2586	3770	8825	6360	3671	8079

ion spray voltage of 4.5 kV and a capillary temperature of 270 or 350 °C. The elemental analyses were performed at the Elemental Analysis Laboratory at the Department of Chemistry, National University of Singapore.

Synthesis. A previously reported procedure was used for the synthesis of target triphenol **1**.[10] The synthetic route is shown in Scheme 1. Ethyl-4-hydroxybenzoate (**2**) and 2-bromophenol (**4**) were protected using benzyl bromide in the presence of K_2CO_3 as the base to give protected phenols **3** and **5**, respectively. 2-Benzyloxy bromobenzene (**5**) was reacted with magnesium (GR grade) in the presence of a catalytic amount of iodine crystals to yield magnesium salt intermediate **6**, which was immediately reacted with 0.5 equiv of benzylated methyl ester (**3**) to give the crude tertiary alcohol **7**. The formation of the tertiary −OH group was confirmed via methylation of the alcoholic group using methyl iodide.[11] Hydrogenolysis of the benzylated derivative using H_2 gas over $Pd(OH)_2$ catalyst gave target triphenol **1**.

Ethyl-4-benzyloxybenzoate (3). Ethyl-4-hydroxybenzoate (**2**) (20 g, 0.12 mol), anhydrous potassium carbonate (50 g, 0.36 mol), and

benzyl bromide (31 g, 0.18 mol) in 1-butanone were refluxed for 24 h. Excess solvent was removed under reduced pressure. The residue was extracted with ether and washed with dilute sodium hydroxide solution and water. The organic layer was dried over anhydrous sodium sulfate, filtered, and concentrated. The crude compound was purified by flash chromatography using hexane/dichloromethane (7:3) as eluents. Colorless liquid, yield 90%. ^{1}H NMR (300 MHz, $CDCl_3$, δ ppm): 1.35 (−C**H**$_3$, t, 3H, J = 6.4 Hz), 4.25 (−C**H**$_2$, q, 2H), 5.08 (Ar−OC**H**$_2$, s, 2H), 6.95 (Ar−**H**, d, 2H, J = 7.2 Hz), 7.23 (Ar−**H**, m, 5H), 7.98 (Ar-**H**, d, 2H, J = 7.2 Hz). ^{13}C NMR (75.4 MHz, $CDCl_3$, δ ppm): 14.6 (−**C**H$_3$), 60.9 (−**C**H$_2$), 70.3 (Ar−O**C**H$_2$), 114.7, 123.5, 127.7, 128.4, 128.9, 131.8, 136.6, 162.7 (Ar−**C**), 166.5 (**C**═O). FT-IR (cm^{-1}): 2976, 2901, 1710, 1602, 1577, 1509, 1421, 1287, 1168, 1003, 849, 765, 696, 654. MS-ESI: m/z 256 (M^+). Elemental Analysis Calcd for $C_{16}H_{16}O_3$: C, 74.98; H, 6.29. Found: C, 74.48; H, 6.30.

2-Benzyloxybromobenzene (5). To a mixture of 25 g (0.14 mol) of 2-bromophenol (**4**) and 40 g (0.28 mol) of anhydrous potassium carbonate in 250 mL of 1-butanone, 37 mL (0.22 mol) of benzyl bromide was added, and the contents of the round-bottom flask were refluxed for 24 h. The solvent was removed under reduced pressure. The residue was extracted with ether and washed with dilute NaOH solution, followed by water. The organic layer was dried over anhydrous sodium sulfate, filtered, and concentrated. The crude product was purified using flash chromatography with hexane/dichloromethane (8:2) as eluents. Colorless oil, yield 90%. ^{1}H NMR (300 MHz, $CDCl_3$, δ ppm): 5.07 (Ar−OC**H**$_2$, s, 2H), 6.78 (Ar−**H**, t, 1H, J = 7.2 Hz), 6.87 (Ar−**H**, d, 1H, J = 7.6 Hz), 7.15 (Ar−**H**, t, 1H, J = 7.2 Hz), 7.2 (Ar−**H**, m, 3H), 7.43 (Ar−**H**, d, 2H, J = 7.6 Hz), 7.52 (Ar−**H**, d, 1H, J = 7.6 Hz). ^{13}C NMR (75.4 MHz, $CDCl_3$, δ ppm): 71.0 (Ar−O**C**H$_2$), 112.8, 114.2, 122.5, 127.3, 127.9, 128, 128.2, 128.7, 128.9, 133.7 (Ar−**C**). FT-IR (cm^{-1}): 2930, 1583, 1477, 1380, 1242, 1161, 1049, 1024, 910, 850, 746, 696, 665, 618. MS-ESI: m/z 262 (M^+) Elemental Analysis Calcd for $C_{13}H_{11}BrO$: C, 59.34; H, 4.21; Br, 30.37. Found: C, 59.82; H, 4.21; Br, 30.37.

Compound 7. Grignard grade magnesium turnings (1.2 equiv. with respect to bromo compound) were placed in a flame-dried three-neck round-bottom (RB) flask. The RB was placed in an ice-bath and a few milliliters of dry THF was added to cover the magnesium turnings. Iodine was added to catalyze the reaction. Approximately 1 equiv of the bromo compound was added to the mixture, and the contents of the RB were warmed until the iodine color disappeared or the contents appeared cloudy. The remaining amount of the bromo compound was added dropwise, and the mixture was warmed till all magnesium turnings were consumed. The mixture was again cooled to 0 °C, and the ester (0.1 equiv) dissolved in dry THF was added dropwise. The solution was heated on a water bath for 6 h and cooled, and a saturated solution of ammonium chloride and crushed ice was added. Extraction was done using diethyl ether; the combined organic layers were washed with brine and water. The organic layer was dried over anhydrous sodium sulfate, filtered, and concentrated. The crude product was purified using flash chromatography with hexane/dichloromethane (6:4) as eluents. Light yellow solid, yield 60%; mp 95 °C. ^{1}H NMR (300 MHz, $CDCl_3$, δ ppm): 4.82 (Ar−OC**H**$_2$, s, 4H), 5.02 (Ar−OC**H**$_2$, s, 2H), 6.81 (Ar−**H**, m, 10H), 7.06 (Ar−**H**, m, 17H). ^{13}C NMR (75.4 MHz, $CDCl_3$, δ ppm): 70.5 (Ar−O**C**H$_2$), 70.6, 81.2 (**C**−OH), 113.3, 114.1, 121, 127.6, 127.9, 128.0, 128.3, 128.6, 129.0, 129.8, 130.1, 135.2, 137.1, 137.7, 156.8, 158.1 (Ar−**C**). FT-IR (KBr, cm^{-1}): 3426, 2909, 1591, 1502, 1423, 1377, 1295, 1020, 856, 785.4, 742, 696. MS-ESI: m/z 578 (M^+). Elemental Analysis Calcd for $C_{40}H_{34}O_4$: C, 83.02; H, 5.92. Found: C, 82.96; H, 5.89.

Bis(2-hydroxyphenyl)-4-hydroxyphenylmethane (1). The benzyl-protected phenol (3 g, 5 mmol) was dissolved in a 1:1 mixture of THF and methanol. One milliliter of water and 20 wt % of $Pd(OH)_2$/C (containing up to 50% of H_2O) were added. The mixture was stirred in the presence of H_2 gas for 4−6 h. Palladium hydroxide was filtered over Celite. The residue was washed with methanol, and the combined filtrates were concentrated to give crude triphenol **1**, which was purified using flash chromatography (hexane/acetone = 8:2). Off-white solid, yield 75%; mp 180 °C. ^{1}H NMR (300 MHz, DMSO-d_6, δ ppm): 5.93 (C−**H**, s, 1H), 6.62 (Ar−**H**, m, 6H), 6.74 (Ar−**H**, d, 4H, J = 7.2 Hz), 6.97 (Ar−**H**, m, 2H), 9.08 (−O**H**, m, 3H). ^{13}C NMR (75.4 MHz, DMSO-d_6, δ ppm): 41.6 (**C**−H), 114.6, 114.7, 118.1, 126.5, 129.4, 130.7, 139.9, 154.6, 155.0 (Ar−**C**). FT-IR (KBr, cm^{-1}): 3523, 3162, 2884, 1590, 1506.9, 1450, 1385, 1329, 1219, 1188, 1090, 1042, 833, 754. MS-ESI: m/z 292 (M^+). Elemental Analysis Calcd for $C_{19}H_{16}O_3$: C, 78.06; H, 5.52 Found C, 78.11; H, 5.40.

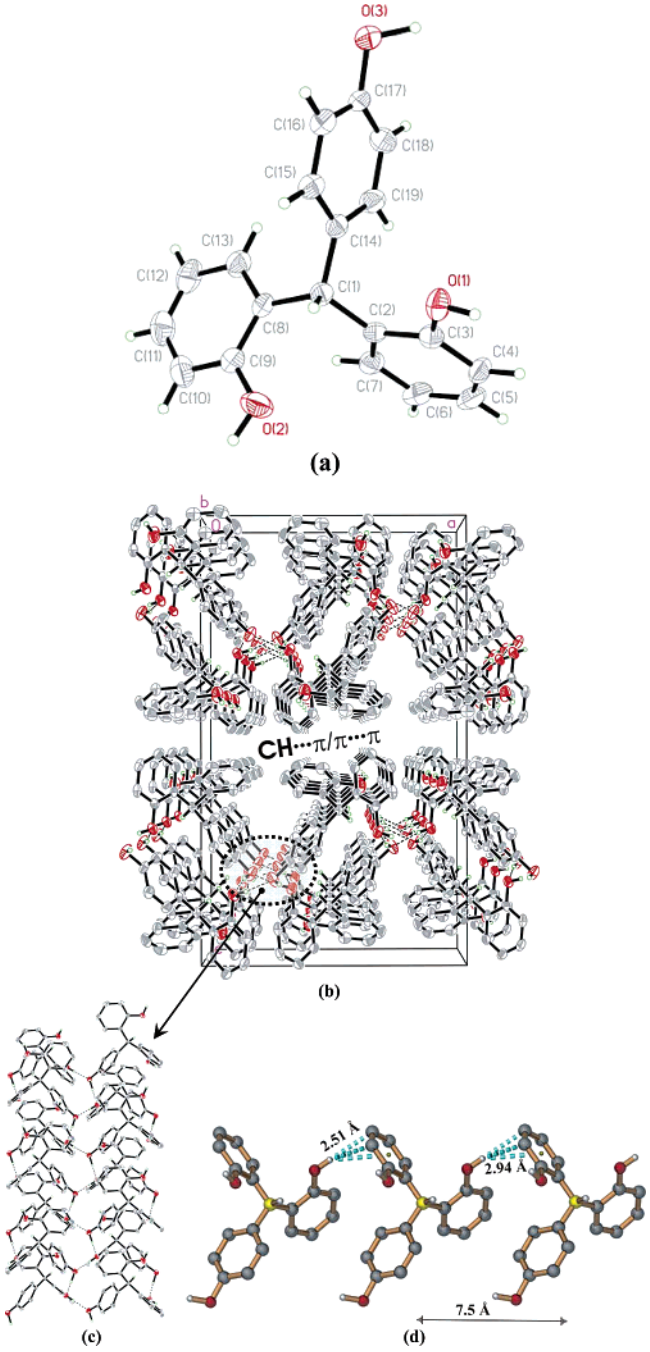

Figure 2. Panel a shows the ORTEP perspective of triphenol **1**. Thermal ellipsoids are drawn at the 50% probability level. Panel b shows the 3D packing arrangement of **1** as viewed along the *b*-axis. Neighboring hydrogen-bonded chains are held together by weak interactions. (c) Molecules of **1** are arranged into distorted ladders in one dimension through cooperative O−H···O hydrogen bonding (green dotted lines). (d) Infinite O−H···π (arene) interactions along the hydrogen-bonded chains are shown as blue dotted lines. Color codes are as follows: C, gray; H, white; O, red; tertiary C, yellow.

Single Crystal X-ray Diffraction. All single crystals were obtained via a slow evaporation technique at ambient conditions in air. Single crystals of triphenol **1** were obtained from a 1:1 mixture of methanol and toluene. The crystals were found to exist in an orthorhombic system with *Pbca* space group. Cocrystallization of triphenol **1** and pyrazine (pyz) from a solution of ethyl acetate gave single crystals of complex **1·pyz**. The crystal structure belongs to the triclinic system and has the space group $P\bar{1}$. Single crystals of **1·phen** (triclinic system, $P\bar{1}$ space

Table 2. Significant Intermolecular Interactions Found in the X-ray Crystal Structure of 1 and Its Adducts[a]

	D−H···A	D−H (Å)	H···A (Å)	D···A (Å)	∠D−H···A (deg)
1	O(1)−H(1A)···O(3)^{i}	0.82(4)	1.87(4)	2.685(4)	173(4)
	O(3)−H(3A)···O(1)^{ii}	1.04(7)	1.70(7)	2.706(4)	162(5)
1·pyz	O(1)−H(1A)···O(2)^{iii}	0.86(2)	1.91(2)	2.762(2)	174(2)
	O(2)−H(2A)···N(1)	0.88(2)	1.85(2)	2.655(2)	151(2)
	C(20)−H(20)···O(1)^{iv}	0.94	2.54	3.351(2)	145
1·phen	O(1)−H(1)···N(3)	0.87(3)	2.07(3)	2.868(3)	152(2)
	O(1)−H(1)···N(4)	0.87(3)	2.54(3)	3.181(3)	131(2)
	O(2)−H(2)···N(2)	0.96(4)	1.83(4)	2.770(3)	165(4)
	O(3)−H(3)···O(1S)	0.92(4)	1.79(4)	2.659(4)	156(4)
	C(22)−H(22)···O(3)^{v}	0.94	2.58	3.320(3)	135
1·bpy	O(1)−H(1A)···N(1)	0.91(3)	1.85(3)	2.726(2)	162(3)
	O(2)−H(2A)···N(3)	0.87(3)	1.88(3)	2.753(2)	175(3)
	O(3)−H(3A)···N(2)^{vi}	0.97(3)	1.78(3)	2.712(3)	160(3)
	C(16)−H(16)···O(3)^{vii}	0.94	2.49	3.342(3)	150
	C(23)−H(23)···O(2)^{viii}	0.94	2.55	3.486(3)	173
1·bpy-ethe	O(1S)−H(1SA)···O(2)	0.91(3)	2.22(5)	3.021(2)	147(5)
	O(1)−H(1A)···N(1)	0.83	1.82	2.635(3)	166
	O(1S)−H(1SB)···O(2)^{ix}	0.91(5)	2.22(5)	3.127(10)	172(6)
	O(2)−H(2A)···O(3)^{x}	0.83	1.90	2.707(3)	165
	O(3)−H(3A)···O(1)^{xi}	0.83	1.88	2.692(2)	167
	C(21)−H(21)···O(1S)^{xii}	0.94	2.39	3.110(2)	133
1·bpy-etha	O(1)−H(1A)···N(1)	0.88(3)	1.88(3)	2.742(3)	166(2)
	O(2)−H(2A)···N(4)	1.09(3)	1.68(3)	2.761(2)	175(3)
	O(3)−H(3A)···N(2)^{xiii}	1.16(4)	1.63(4)	2.764(3)	165(3)

[a] Symmetry operators: (i) $^1/_2 + x, y, ^3/_2 - z$ (ii) $1 - x, ^1/_2 + y, ^3/_2 - z$ (iii) $x, -1 + y, z$ (iv) $-x, 1 - y, 1 - z$ (v) $x, -1 + y, z$ (vi) $1 - x, -y, 1 - z$ (vii) $2 + x, ^1/_2 - y, ^1/_2 + z$ (viii) $-1 + x, y, z$ (ix) $-x, 2 - y, -z$ (x) $x, -1 + y, z$ (xi) $1 - x, 1 - y, -z$ (xii) $-x, 1 - y, -z$ (xiii) $1 - x, 2 - y, 1 - z$.

group) were obtained from a solution containing a mixture of THF/CH_3CN (1:1) as monohydrate; however, hydrogen atoms of the water molecules could not be located. Crystals of **1·bpy**, which exists in the monoclinic system with $P2_1/c$ space group, were collected from acetonitrile solution. A mixture of THF/MeOH (1:1) yielded colorless crystals of **1·bpy-ethe** monohydrate in $P\bar{1}$ space group. Slow evaporation from a solution of methanol and THF (1:1) containing stoichiometric amounts of **1** and bpy-etha resulted complex **1·bpy-etha** in $P\bar{1}$ space group.

Good quality single crystals were carefully chosen and glued onto a thin glass fiber. X-ray diffraction data on single crystals were collected on a Bruker AXS SMART CCD three-circle diffractometer with Mo Kα radiation ($\lambda = 0.710\,73$ Å) at 23 °C. The software used was SMART[12] for collecting frames of data, indexing reflections, and determining lattice parameters, SAINT[12] for integration of intensity of reflections and scaling, SADABS[13] for absorption corrections, and SHELXTL[14] for space group determination, structure solution, and least-squares refinements on F^2. Structures were solved by direct methods and non-hydrogen atoms were refined anisotropically. Hydrogen atoms were introduced at fixed distances from carbon atoms and assigned fixed thermal parameters. The hydrogen atoms attached to the oxygen were refined isotropically. All H-atoms could not be located in complex **1·phen**. All calculations were performed on a Silicon Graphics workstation, using programs provided by Siemens Pvt. Ltd.

Crystal data and structural refinement parameters of triphenol **1** and its aza complexes are given in Table 1.

Results and Discussion

Solid State Self-Assembly of Triphenol 1. The asymmetric unit in the crystal structure consists of one molecule of the triphenol. The ORTEP representation and atom-labeling scheme of triphenol **1** are shown in Figure 2a.

In the crystal lattice of **1**, the molecules are linked via O−H···O hydrogen bonds with a distorted ladder-type motif in 1D. The ladder arises from the participation of the hydroxyl groups from the neighboring chains as shown in Figure 2b,c.[15] Along the hydrogen-bonded ladder, each hydroxyl group is hydrogen-bonded to two neighboring molecules. Thus the para hydroxyl group and one of the ortho hydroxyl groups of triphenol **1** participates in the formation of infinite O−H···O hydrogen bonds [H1A···O3 1.87(4) Å, 173(4)° at $(^1/_2 + x, y, ^3/_2 - z)$; H3A···O1 1.70(7) Å, 162(5)° at $(1 - x, ^1/_2 + y, ^3/_2 - z)$] (Figure 2c). The other ortho hydroxyl group that does not participate in O−H···O hydrogen bonds is involved in O−H···π interactions (edge-to-face, H2A···C_g1, 2.94 Å, 146° at $(^1/_2 + x, y, ^3/_2 - z)$; with closest contact edge-to-edge O2−H2A···π(C5−C4) 2.51−2.61 Å; C_g1 C_2−C_7. C_g refers to the ring center of gravity) along the H-bonded chain direction (Figure 2d). The O−H···π interactions are directed toward the edge rather the centroid of the arene ring.[2g] The neighboring hydrogen-bonded chains are held together via C−H···π (2.8−3.2) Å and π···π stacking interactions (3.48 Å), Figure 2b as viewed along the *b*-axis. The hydrogen bond distances and angles are given in Table 2.

Solid-State Self-Assembly of 1·pyz. The ORTEP representation and atom labeling scheme of **1·pyz** are given in Figure 3a. Molecular recognition in **1·pyz** between triphenol and pyrazine primarily occurs through O−H···N bonds, which result in the formation of ladder-type assemblies. In such a recognition pattern, the molecules of **1** are held together by O−H···O hydrogen bonds [O1A−H1A···O2 1.91(2) Å, 174(2)°], which form the rods of the ladder (Figure 3b). The molecular rods are separated by a distance of ca. 8 Å. The **pyz** molecules and one of the phenyl rings of **1** are inserted between the rods as rungs, and **pyz** units are held together by O−H···N [O2A−H2A···N1 1.85(2) Å, 151(2)°] hydrogen bonds. The repeating **pyz** units along the rungs are separated by ca. 10 Å, and the molecules along the ladder are stabilized by π···π stacking interactions with a center-to-center (aza/arene) distance of 4.11 Å (close contact 3.19 Å). Ladders of the type shown in Figure 3b interact with adjacent H-bonded ladders through C−H···O hydrogen bonds [C20−H20···O1 2.54 Å, 145°] (Figure 3c).

One of the ortho hydroxyl groups of the triphenol that does not participate in O−H···O hydrogen bonding is involved in O−H···π interactions (2.98 Å) with the phenyl rings of the neighboring molecules (Figure 3d).[2g] These interactions with the neighboring triphenol ring are of the "edge" rather than the "centroid" type. In addition, along the hydrogen-bonded ladder, the adjacent rods are stabilized by C−H···π interactions, 2.73 Å (Figure 3d).

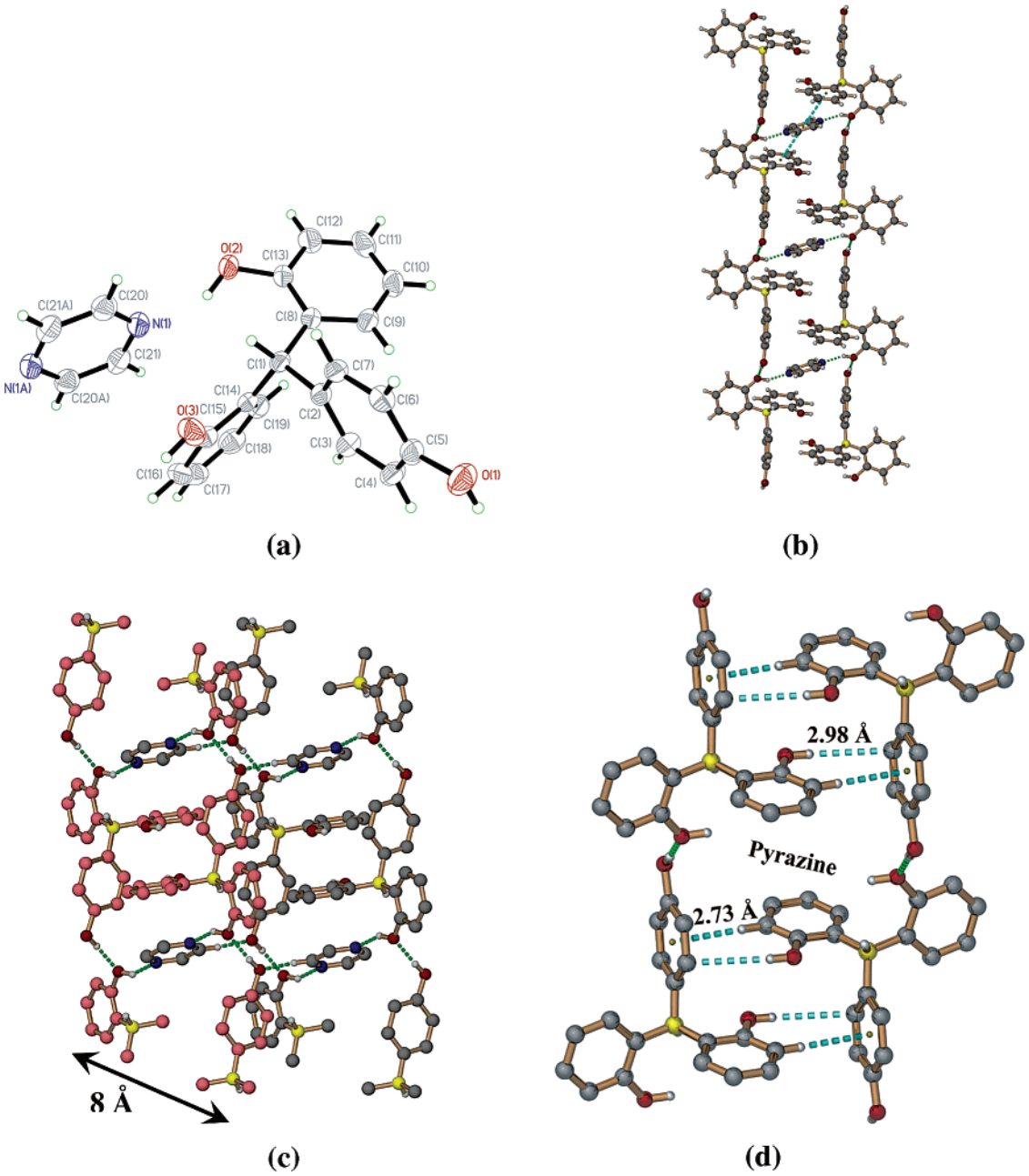

Figure 3. Panel a shows the ORTEP perspective of complex **1·pyz**. Thermal ellipsoids are drawn at 50% probability level. Color codes are as follows: C, gray or yellow; H, white; O, red; N, blue. In panel b, ladder-type structures are formed between **1** and pyrazine. The pyrazine molecules are involved in the formation of rungs and are separated by ca. 10 Å; $\pi\cdots\pi$ stacking interactions (4.11 Å) are shown by blue dotted lines. Panel c shows packing of neighboring ladders through O−H···N and C−H···O hydrogen bonds between the layers. Neighboring rods have been coded pink and gray. Panel d shows a view of C−H···π/O−H···π interactions (blue dotted lines) [C16−H16···π (C2−C7) 2.73 Å, 176° at ($1-x$, $2-y$, $1-z$); O3−H3A···C3 2.98 Å, 178° at ($1-x$, $1-y$, $1-z$)]. The pyrazine unit in panel d is removed for clarity. Tertiary C atoms are coded yellow. Some H atoms bonded to carbon have been omitted for clarity. The strong hydrogen bonds are represented by green dotted lines.

Solid-State Self-Assembly of 1·phen. The ORTEP perspective and atom labeling scheme of **1·phen** are given in Figure 4a. All hydrogen atoms could not be located in the crystal structure.

The molecules of **1** and phenanthroline are linked to form a three-dimensional framework by a combination of O−H···N and C−H···O hydrogen bonds. Two independent O−H···N hydrogen bonds generate a one-dimensional substructure in the form of hydrogen-bonded chains. Atoms N3 and N4 of the phenanthroline act as H-bond acceptors to atom O1 [O1−H1···N3 2.07(3) Å, 152(2)°; O1−H1···N4 2.54(3) Å, 131(2)°]. N2 acts as an acceptor to O2 of the triphenol [O2−H2···N2 1.83(4) Å, 165(2)°], Figure 4b. Atom O3 of the triphenol acts as donor to O1S of the THF molecule [O3−H3···O1S 1.79(4) Å, 156(4)°] (Figure 4b) and simultaneously serves as acceptor to the adjacent molecule of 1,10-phenanthroline via weak C−H···O hydrogen bonds (C22−H22···O3 2.58 Å, 135°; Table 2). The triphenol molecules interact with one another through C−H···π (2.93 Å) interactions leading to the formation of a closed elliptical network with cross-section of ca. $\sim 8 \times 12$ Å^2. The molecules of 1,10-phenanthroline that fill these spaces are stabilized via $\pi\cdots\pi$ and C−H···π interactions (Figure 4c). 1,10-Phenanthroline rings are aligned parallel but in inverse fashion with a plane-to-plane distance of 3.6−3.9 Å (Figure 4b). The THF molecules are stabilized through edge-to-face C−H···π interactions (2.64−3.31 Å) as shown in Figure 4d.

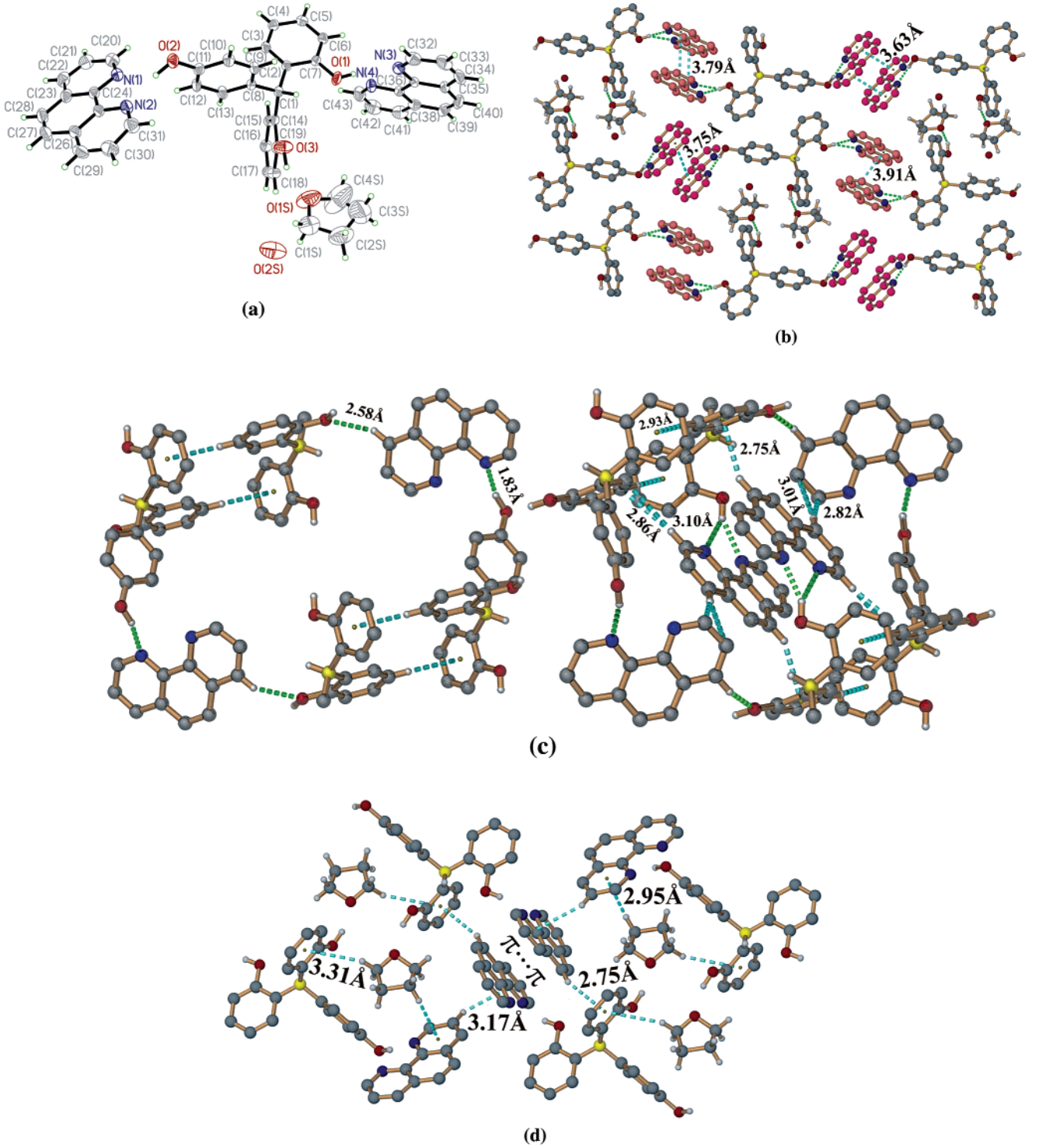

Figure 4. Panel a shows the ORTEP perspective of complex **1·phen**. Thermal ellipsoids are drawn at 50% probability level. Color codes are as follows: C, gray; H, white; O, red; N, blue. Panel b shows part of the crystal structure of complex **1·phen** showing the formation of 1D H-bonded chains; $\pi\cdots\pi$ stacking interactions (blue dotted lines) link the chains. The phenanthroline molecules that are involved in $\pi\cdots\pi$ interactions are shown in pink color. Panel c shows the elliptical cavity formation and occupation of the cavity by 1,10-phenanthroline in a two-dimensional arrangement involving weak interactions. Panel d shows edge-to-face C−H$\cdots\pi$ interactions (shown by blue dotted lines) with THF molecules. For clarity, some H atoms bonded to carbon have been omitted. Strong hydrogen bonds are represented by green dotted lines; tertiary carbon is coded in yellow.

Solid-State Self-Assembly of 1·bpy. The ORTEP representation and atom labeling scheme of the complex **1·bpy** are shown in Figure 5a. Two −OH groups of the triphenol molecule (O1 and O3) are hydrogen-bonded to bpy molecules via O−H···N bonds [O1−H1A···N1 1.85(3) Å, *d*(O···N) 2.726 (2) Å, 162(3)°; O3−H3A···N2 1.78(3) Å, *d*(O···N) 2.712 Å, 160(3)°], which together with C−H···O interactions [C16−H16···O3 2.49 Å, 150°] forms a large hypothetical cavity of dimension ∼15 × 18 Å^2 (Figure 5b). Figure 5b can be best described as hydrogen-bonded sheets resembling a herringbone pattern consisting each of four bpy and six triphenol molecules. A single unit resembles a pseudo-cyclohexane type structure (Figure 5b, insert). The wave-type structure is nonplanar and forms an infinite undulating 2D sheet-type structure in the lattice. Identical

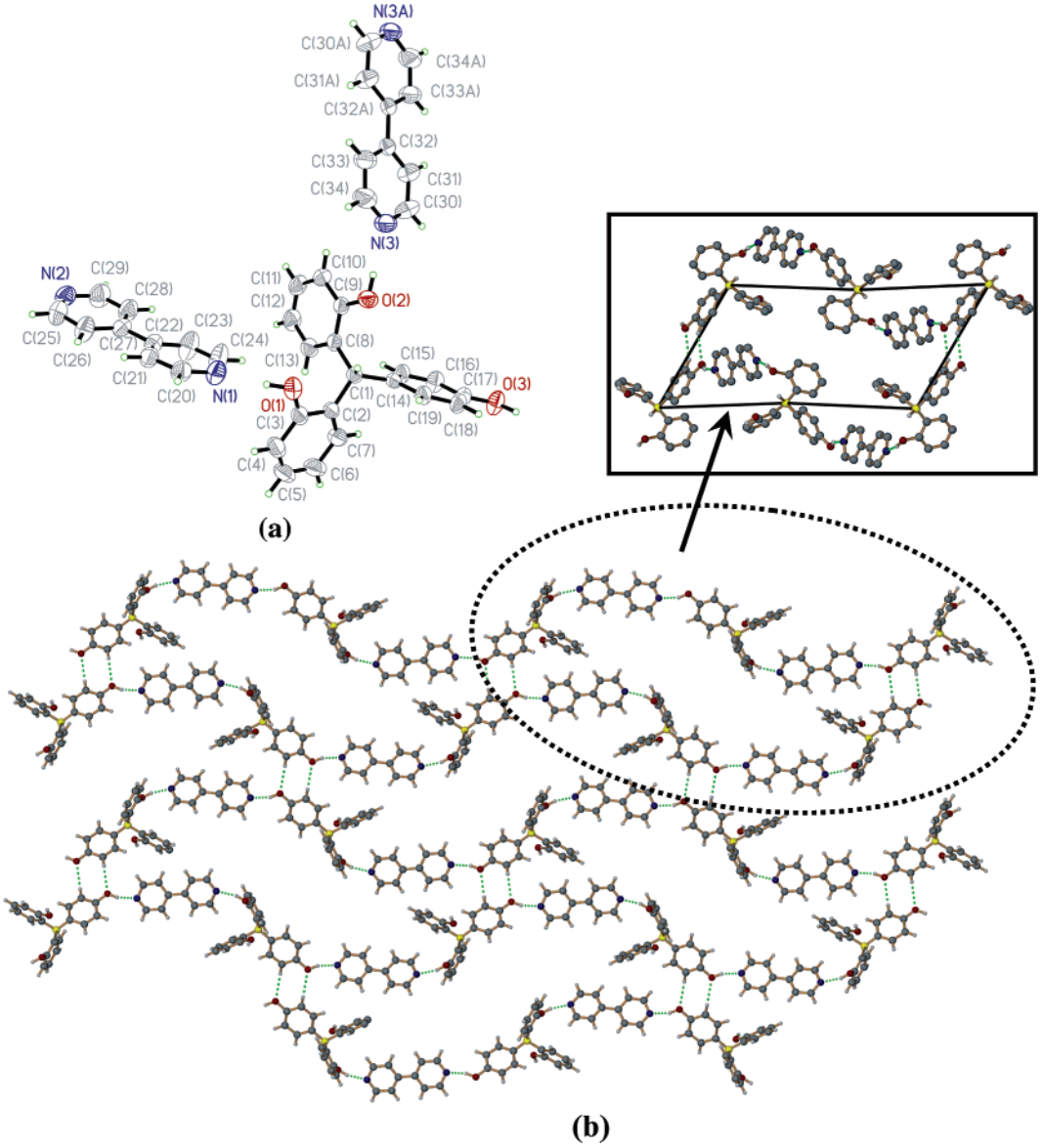

Figure 5. Panel a shows the ORTEP perspective of complex **1·bpy**. Thermal ellipsoids are drawn at 50% probability level. Panel b shows the molecular recognition between **1** and bpy through O−H···N and C−H···O interactions leading to the formation of hydrogen-bonded herringbone-type structure (inset shows a pseudo-cyclohexane-type structure formed between bpy and triphenol). Color codes are as follows: C, gray; H, white; O, red; N, blue; tertiary C, yellow. For clarity H atoms bonded to carbon have been omitted. The hydrogen bonds are represented by dotted lines (coded green).

hydrogen-bonded sheets stack over each other and are stabilized by C−H···O hydrogen bonds (C23−H23···O2 2.55 Å, 173°). Apart from the strong hydrogen bonds, the layers are also stabilized by off-shifted $\pi\cdots\pi$ interactions (4.58 Å).[16] The distance between the centroids, aza/aza and aza/arene, are 4.15 and 4.41 Å, respectively. The spaces are filled with the second bpy molecule (involving nitrogens N3 and N3A) that is involved in interpenetration.

The most interesting feature of the complex is that a 4-fold interpenetrating 3D structure is generated through the third OH group (O2−H2) of the triphenol that orients into the cavity. The O2−H2 from the first hydrogen-bonded sheet penetrates through three other sheets and interacts with the bpy molecules [O2−H2A···N3 1.88(3) Å, 175(3)°] resulting in a fourfold interpenetrating structure. Weak C−H···π interactions also stabilize the 3D network [C20−H20···C_g2 2.89 Å, 161° at ($-x$, $^1/_2 + y$, $^1/_2 - z$); C30−H30···C_g4 3.05 Å, 138° at ($-x$, $-^1/_2 + y$, $^1/_2 - z$), where C_g2 involves C_8−C_{13} and C_g4 involves N_1 and C_{20}−C_{24}]. The hydrogen-bond distances and angles are given in Table 2.

Solid-State Self-Assembly of 1·bpy-ethe. X-ray structure determination reveals that the complex **1·bpy-ethe** exists as a monohydrate. The ORTEP representation and atom labeling scheme of the complex **1·bpy-ethe** are shown in Figure 6a.

The recognition between the phenol and diamine occurs primarily through O−H···N, O−H···O, and C−H···O hydrogen bonds (Table 2). In the crystal lattice, the molecules of **1** are held together by O−H···O hydrogen bonds (both from the phenol and from water) to yield ladder-type architectures. The organized triphenol and water molecules serve as the rods of the ladder. The O−H···O hydrogen bond distances and angles are as follows: O1S−H1SA···O2 2.22(5) Å, 147(5)°; O1S−H1SB···O2 2.22(5) Å, 172(6)°; O3−H3A···O1 1.88 Å, 167°; O2−H2A···O3 1.90 Å, 165° (Figure 6b). The rods of the ladders are separated by a distance of ∼8 Å (Figure 6c). The bpy-ethe molecules are inserted between the rods as rungs. The molecules

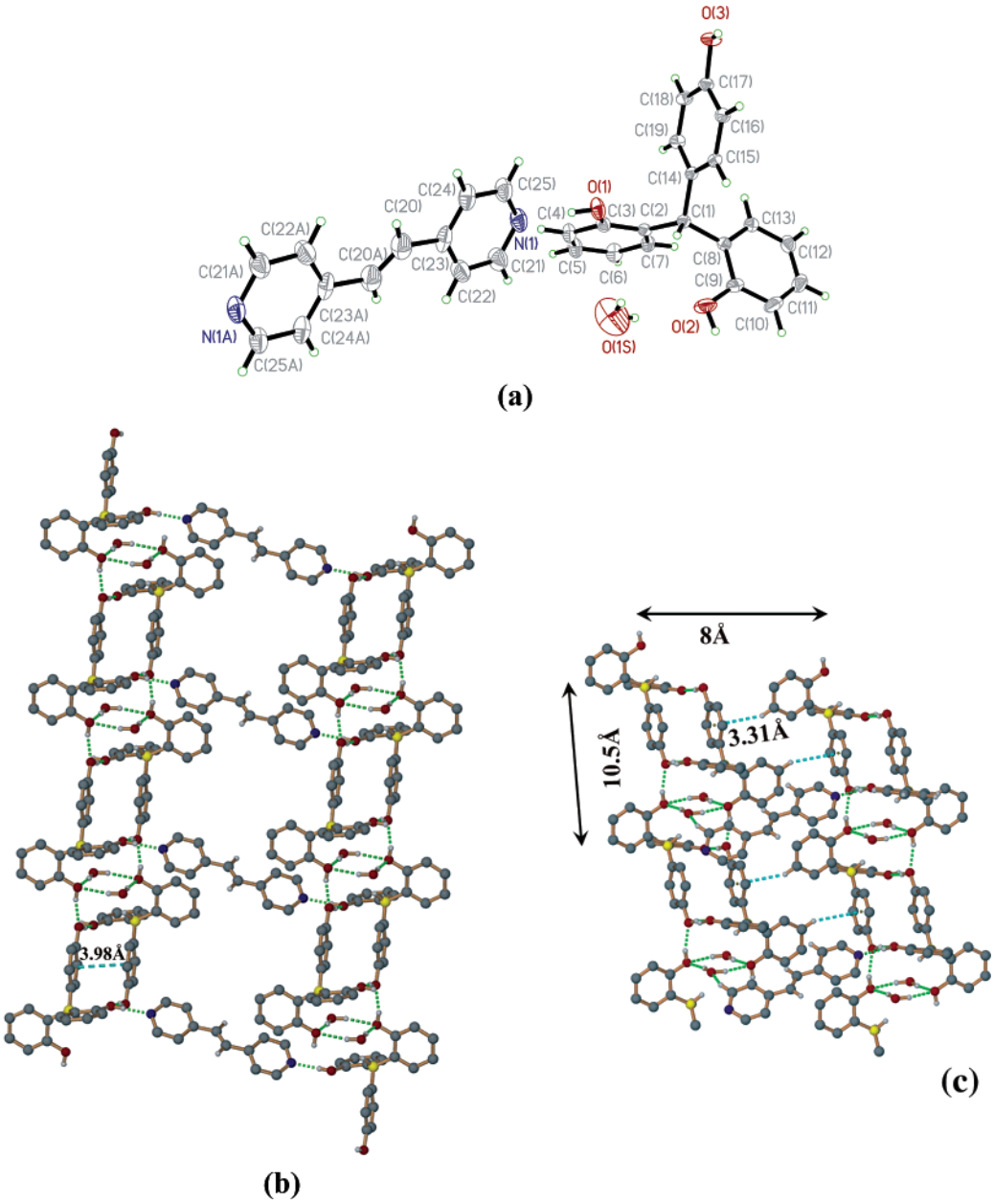

Figure 6. Panel a shows the ORTEP representation of complex **1·bpy-ethe**. Thermal ellipsoids are drawn at 50% probability level. Color codes are as follows: C, gray or yellow; H, green or white; O, red; N blue. Panel b shows the molecular recognition between **1** and bpy-ethe through O−H···N and C−H···O interactions leading to the formation of the hydrogen-bonded molecular ladder. Strong hydrogen bonds are represented by green dotted lines. Panel c shows the C−H···π interactions (coded blue) between the neighboring hydrogen-bonded rods. H atoms bonded to carbon have been omitted for clarity.

of **1** interact with bpy-ethe molecules through O−H···N hydrogen bonds (O1−H1A···N1 1.82 Å, 166°) as shown in Figure 6b. The rungs (bpy-ethe molecules) are separated by a distance of ca. 10.5 Å. The bpy-ethe molecules interact with neighboring rods via C−H···O hydrogen bonds with water (C21−H21···O1S 2.39 Å, 133°). Neighboring triphenol molecules along the ladder are hydrogen-bonded to form boxes that are stabilized by $\pi\cdots\pi$ interactions. The distance between the centroids (arene/arene) is 3.97 Å. The adjacent stacks of rods together with the bpy-ethe molecules are stabilized by C−H···π interactions[17] [^{i}C5−H5···C_g2 2.93 Å, 148°; ^{ii}C10−H10···C_g4 3.33 Å, 123°; ^{iii}C12−H12···C_g3 3.31 Å, 156°; ^{iv}C18−H18···C_g4 3.23 Å, 125°; ^{v}C22−H22···C_g1 3.10 Å, 141°; ^{vi}C24−H24···C_g2 3.09 Å, 140°, where C_g1 involves C_2−C_7, C_g2 C_8−C_{13}, C_g3 C_{14}−C_{19}, and C_g4 N_1 and C_{21}−C_{25}. Symmetry operators are (i) $1 + x, y, z$, (ii) $-x, 1 - y, -z$, (iii) $-x, 2 - y, -z$, (iv) $1 - x, 2 - y, -z$, (v) $1 - x, 1 - y, -z$, and (vi) $x, y, -1 + z$] (Figure 6c).

Solid-State Self-Assembly of 1·bpy-etha. The ORTEP representation of the complex **1·bpy-etha** and atom labeling scheme are given in Figure 7a. The bpy-etha molecules exist in both trans and gauche conformations in the lattice.

The triphenol and bpy-etha molecules recognize each other through the formation of O−H···N hydrogen bonds [O1−H1A···N1 1.88(3) Å, 166(2)°; O3−H3A···N2 1.63(4) Å, 165-(3)°] (Table 2). The net result of the O−H···N bonding is the formation of a rectangular grid with a dimension of ca. ∼14 × 10 Å^2 (Figure 7b). The ethane moiety of the bpy-etha molecules involved in the formation of the rectangular grid is in gauche conformation with a torsion angle of −58° (C29−C20−C21−C24). The rectangular grids are separated by a distance of ca. ∼11.4 Å, and the neighboring grids are stabilized by C−H···π

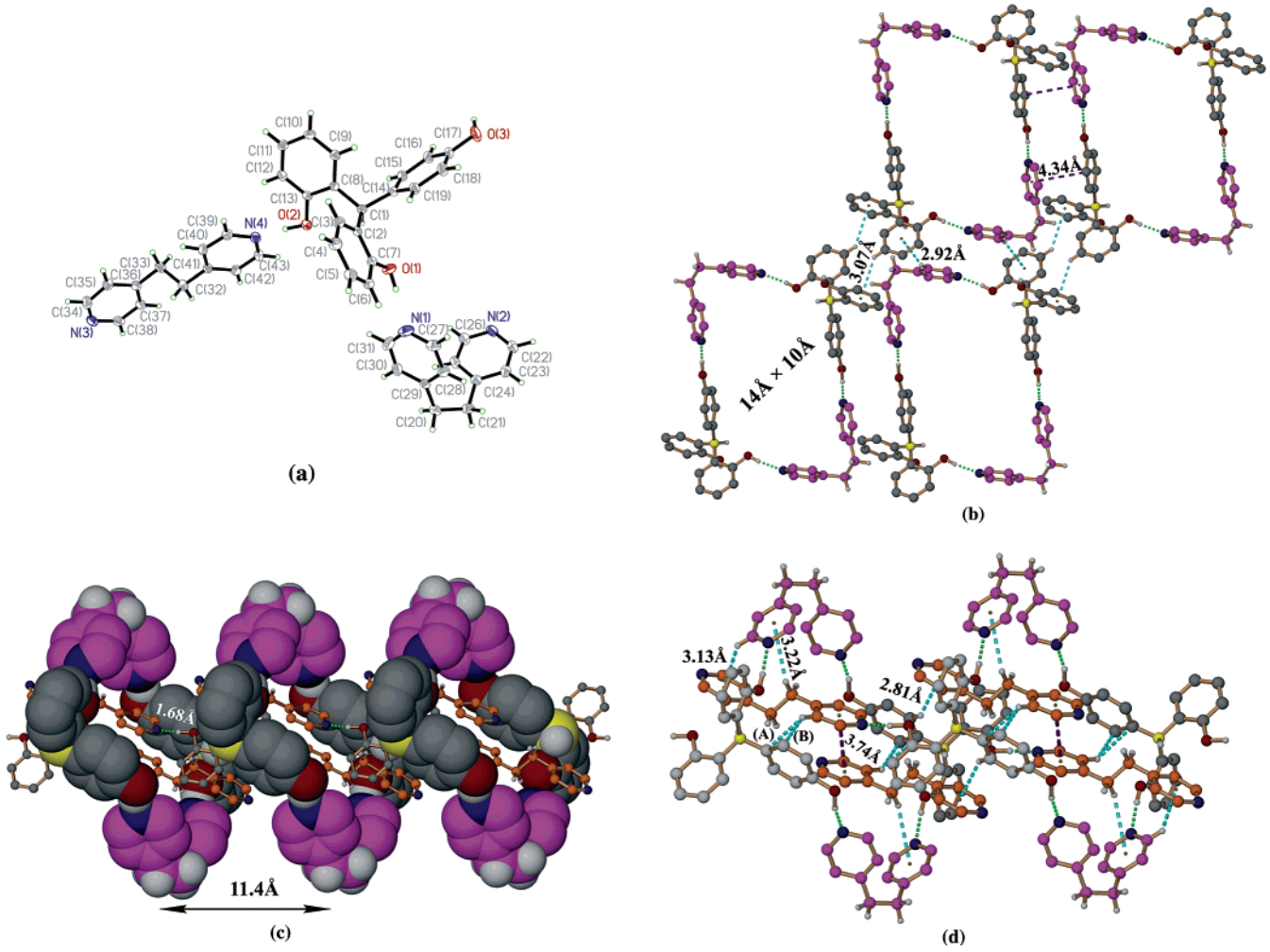

Figure 7. Panel a shows the ORTEP diagram of complex **1·bpy-etha**. Thermal ellipsoids are drawn at the 50% probability level. Selected torsional angles are C24−C21−C20−C29 = −54.9° and C41−C32−C33−C36 = −174.8°. Color codes are as follows: C, gray or yellow; O, red; N, blue; H, white. Panel b shows the formation of rectangular grid (∼14 × 10 Å^2) between the triphenol molecules and bpy-etha in gauche conformation. Also shown are C−H···π interactions between neighboring grids: ^{i}C4−H4···C_g2 3.07 Å, 143°, where C_g2 involves C_8−C_{13} at (2 − *x*, 1 − *y*, −*z*). Panel c displays the space-filling representation showing the occupation of the cavity by another bpy-etha molecule (trans conformation). Panel d shows the O−H···N, C−H···π, and π···π interactions. Edge-to-edge interactions are labeled as follows: (A) C40−H40A···C19 3.17 Å, 139°; (B) C40−H40A···C14 3.01 Å, 148°, at (*x* − 1, *y*, *z*). Edge-to-face interactions are as follows: ^{i}C37−H37···C_g2 2.87 Å, 130°; ^{i}C15−H15···C_g6 2.81 Å, 144°; ^{ii}C32−H32A···C_g4 3.22 Å, 150°; ^{iii}C31−H31···C_g6 3.14 Å, 129°, where C_g2 involves C_8−C_{13}, C_g4 N_1 and C_{27}−C_{31}, and C_g6 N_3 and C_{34}−C_{38}. Symmetry operators are as follows: (i) 3 − *x*, 2 − *y*, 1 − *z*; (ii) 2 − *x*, 2 − *y*, 1 − *z*; (iii) −1 + *x*, *y*, *z*. H atoms bonded to carbon have been omitted for clarity. Strong hydrogen bonds are shown by green dotted lines. The bpy-etha molecules in the gauche conformation (involved in formation of the grid) are coded in purple, while those in trans are coded in orange.

interactions (2.91−2.99) Å as shown in Figure 7b,c. In addition to the above interactions, the neighboring grids are also stabilized via π···π stacking interactions. The distance between the centroids (aza/aza) is 4.34 Å. The O2 atom of the hydroxyl group acts as a hydrogen-bond donor to the nitrogen atom N4 of the second bpy-etha molecule (trans conformation) [O2−H2A···N4 1.68(3) Å, 175(3)°]. The other end of the bpy-etha molecule penetrates through the hydrogen-bonded rectangular grid (Figure 7c).

The nitrogen atom N3 of bpy-etha has no acceptor and is stabilized by C−H···π interactions within the grids (H15···π 2.18 Å, 144°; Figure 7d). In addition to the above interaction, the H-atom of ethane moiety in bpy-etha interacts through C−H···π interaction [C32−H32A··C_g6 3.21 Å, 150° at (2 − *x*, 2 − *y*, 1 − *z*), where C_g6 involves N_3 and C_{34}−C_{38}]. The threading of the bpy-etha molecules through the rectangular grid is achieved by the existence of π···π stacking interactions. The distance between the centroids (aza/aza) is 3.74 Å. Further, the adjacent molecules of **1** as well as bpy-etha molecules interact with the trans form of bpy-etha through C−H···π interactions as shown in Figure 7d. This is an interesting case in which one of the reactant molecules exists as an entrapped guest within the cavity formed in the crystal lattice (Figure 7c). Analysis of π···π stacking interactions in the phenol−aza adducts is given in Table 3.

Comparison of the Packing Motifs

The principles of self-assembly have been successfully utilized in the design of novel molecular assemblies using a triphenol building block. A schematic representation showing the general packing of the molecules in the crystal lattice of the complexes is given in Figure 8. Triphenol **1** crystallizes into ladder-type networks held together by O−H···O hydrogen bonds (Figure 8a). The packing of the molecule in 3D is similar to the previously reported trisphenols.[10a] The lattice of **1·pyz** is characterized by a ladder structure formed via the interplay of C−H···O and O−H···N bonds. The triphenol serves as the rods,

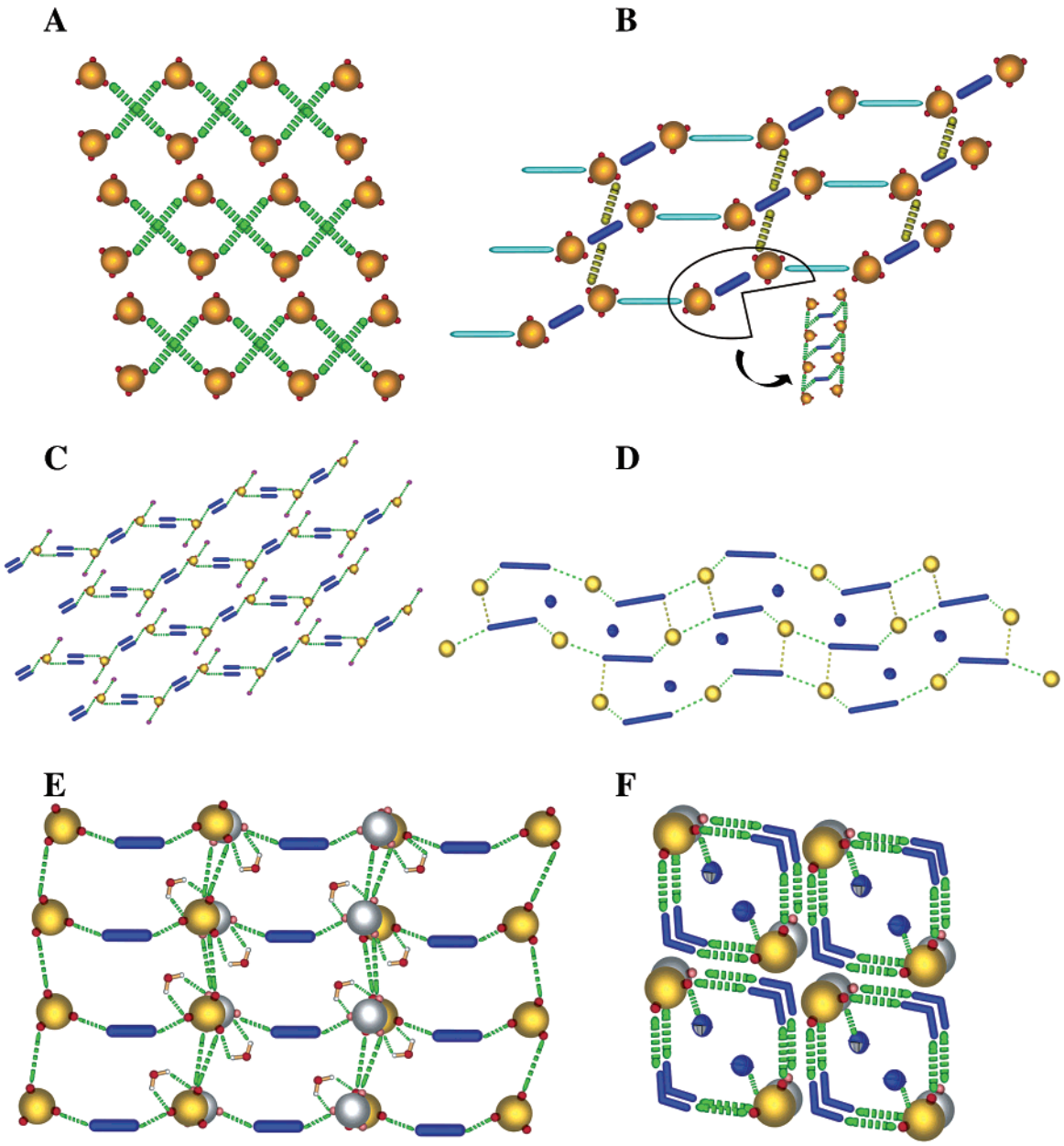

Figure 8. Schematic representation of the general packing arrangements in (A) triphenol **1** and (B) **1·pyz** (the light blue lines represent weak hydrogen bonds; the yellow dotted lines indicate the existence of C−H···O interactions), (C) **1·phen**, (D) **1·bpy**, and (E) **1·bpy-ethe** (water molecules are shown as wedges with oxygen as red spheres and hydrogen as white spheres), and (F) **1·bpy-etha**. Molecules of bpy-etha and bpy involved in interpenetration are shown by blue spheres. The yellow and gray spheres represent the triphenol molecules; the aza compounds are shown as blue rods. Hydrogen bonds are shown by green dotted lines.

while the pyz units behave as rungs of the ladders. One of the phenyl rings of **1** is associated through weak C−H···π interactions with the neighboring rods (Figure 8b). Complex **1·phen**, which also involves a rigid amine, self-assembles into linear H-bonded chains as shown in Figure 8c. The phen molecules are stabilized via π···π stacking and the solvent molecules (THF), through weak C−H···π interactions. Interpenetrating wave-type structures were observed in the crystal lattice of **1·bpy** (Figure 8d). The absence of flexible spacers between the pyridyl moieties leads to the formation of interpenetrating structures. Complexation of **1** with flexible diamines led to changes in free volume in the lattice resulting in extended ladder-type assemblies in **1·bpy-ethe**. The phenolic molecules together with water serve as rods of the ladder, while the bpy-ethe units are inserted as rungs (Figure 8e). Complex **1·bpy-etha** represents a unique wheel and axle type supermolecule. The bpy-etha molecules exist in both trans and gauche conformations in the lattice. The gauche form of bpy-etha interacts with **1** through O−H···N bonds to form rectangular grids into which a second bpy-etha molecule (trans) slides through to form a close-packed lattice (Figure 8f).

Conclusion

The self-assembly of triphenol **1** and its supramolecular complexes with aza compounds has been described. Pyrazine, which represents the smallest rigid spacer, interacts with triphenol **1** to form ladder-type structures. One of the hydroxyl groups is involved in O−H···π interactions. Infinite hydrogen-bonded chains predominate the crystal lattice constructed from the rigid 1,10-phenanthroline and triphenol (**1·phen**). Complexation of **1** with bpy generates a fourfold interpenetrating structure

Table 3. Summary of $C_g\cdots C_g$, Interplanar Distances (Å) and Angles α and γ (deg) for Triphenol 1 and Its Adducts

	ring centroids	$C_g\cdots C_g$[a] (Å)	interplanar distance[b] (Å)	α[c] (deg)	γ[d] (deg)
1·pyz	$C_g4-C_g3^{i}$	4.117(1)	3.053	25.48	28.35
1·phen	$C_g4-C_g5^{ii}$	3.630(2)	3.497	4.07	13.92
	$C_g6-C_g6^{ii}$	3.747(2)	3.447	0.00	23.10
	$C_g7-C_g8^{iii}$	3.794(2)	3.529	1.44	21.47
	$C_g9-C_g9^{iii}$	3.910(1)	3.506	0.04	26.29
1·bpy	$C_g1-C_g6^{iv}$	4.586(1)	3.598	42.36	50.64
	$C_g4-C_g5^{v}$	4.155(1)	3.505	10.04	29.01
	$C_g5-C_g3^{vi}$	4.413(1)	3.707	38.31	46.33
1·bpy-ethe	$C_g3-C_g3^{vii}$	3.975(1)	3.310	0.00	33.61
1·bpy-etha	$C_g5-C_g4^{viii}$	4.337(1)	4.020	32.88	30.73
	$C_g7-C_g7^{ix}$	3.745(1)	3.474	0.00	21.95

[a] Intercentroid distance, C_g refers to the ring center of gravity. The numbers represent the aromatic rings involved in the interaction. [b] Perpendicular distance between the mean planes of two rings. [c] Dihedral angle between the mean planes of two rings. [d] Angle between the centroid of the first ring and normal to the mean plane of the second ring: (i) C_g3 C14−C19; C_g4 N1, C20−C21; $1-x, 2-y, 1-z$ (ii) C_g4 N1, C20−C24; C_g5 N2, C25−C31; C_g6 C23−C28; $2-x, 1-y, -z$ (iii) C_g7 N3, C32−C36; C_g8 N4, C37−C43; C_g9 C35−C40; $1-x, 3-y, 1-z$. (iv) C_g1 C2−C7; C_g6 N3, C30−C34; $x, {}^1/_2-y, {}^1/_2-z$. (v) C_g4 N1, C20−C24; C_g5 N2, C25−C29; $1+x, y, z$. (vi) C_g3 C14−C19; $-1+x, {}^1/_2-y, {}^1/_2+z$. (vii) C_g3 C14−C19; $-x, 2-y, -z$. (viii) C_g3 C14−C19; C_g5 N4, C39−C43; $x, y, 1+z$ (ix) $3-x, 2-y, 1-z$.

with characteristic herringbone motifs observed in two dimensions. Introduction of flexible **1·bpy-ethe** molecules increased the free volume in the lattice to accommodate complex ladder-type architectures. Lattice expansion was further facilitated in **1·bpy-etha** enabling large reactant molecules of bpy-etha (trans) to occupy voids in the structure.

Such investigations pertaining to complexes formed from rigid 3D triphenols with rigid/flexible aza compounds help to understand the possible molecular assemblies that may be formed in systems involving multiple competitive forces. A rationale for the observed results is provided.

Acknowledgment. The authors thank Prof. Koh Lip Lin and Ms. Tan Geok Kheng for their assistance in data collection and structure refinements. We thank the National University of Singapore for financial support. All technical support from various laboratories at the Department of Chemistry, National University of Singapore, is acknowledged.

Supporting Information Available: Details of crystal coordinates and torsion angles for **1**, **1·pyz, 1·phen**, **1.bpy**, **1.bpy-ethe**, and **1.bpy-etha** as CIF files. This material is available free of charge via the Internet at http://pubs.acs.org.

References

(1) (a) Steed, J.; Atwood, J. L. *Supramolecular Chemistry*; John Wiley & Sons: New York, 2000. (b) Desiraju, G. R. *Crystal Engineering, The Design of Organic Solids*; Elsevier: Amsterdam, 1989. (c) Aakeröy, C. B.; Beatty, A. M. *Aust. J. Chem*. **2001**, *54*, 409. (d) Zhang, X. L., Chen, X.-M. *Cryst. Growth Des*. **2005**, *5*, 617. (e) MacDonald, J. C.; Dorrestein, P. C.; Pilley, M. M. *Cryst. Growth Des*. **2001**, *1*, 29. (f) Du, M.; Zhang. Z.-H.; Zhao, X.-J. *Cryst. Growth Des*. **2005**, *5*, 1199. (g). Olenik, B.; Smolka, T.; Boese, R.; Sustmann, R. *Cryst. Growth Des*. **2003**, *3*, 183. (h) Reddy, L. S.; Nangia, A.; Lynch, V. M. *Cryst. Growth Des*. **2004**, *4*, 89. (i) Du, M.; Zhang. Z.-H.; Zhao, X.-J. *Cryst. Growth Des*. **2005**, *5*, 1247.

(2) (a) Melendez, R.; Hamilton, A. *Top. Curr. Chem*. **1998**, *198*, 97. (b) Prins, L. J.; Neuteboom, E. E.; Parachiv, V.; Calama-Crego, M.; Timmerman, P.; Reinhoudt, D. N. *J. Org. Chem*. **2002**, *67*, 4808. (c) Campbell, K.; Kuehl, C. J.; Ferguson, M. J.; Stang, P. J.; Tykwinski, R. R. *J. Am. Chem. Soc*. **2002**, *124*, 7266. (d) Tessa ten Cate, A.; Sijbesma, R. P. *Macromol. Rapid. Commun*. **2002**, *23*, 1094. (e) Nangia, A.; Desiraju, G. R. *Top. Curr. Chem*. **1998**, *98*, 57. (f) Biradha, K. *CrystEngComm* **2003**, *5*, 374. (g) Brehmer, T. H., Weber, E., Cano, F. H. *J. Phys. Org. Chem*. **2000**, *13*, 63.

(3) (a) Suezawa, H.; Yoshida, T.; Hirota, M.; Takahashi, H.; Umezawa, Y.; Honda, K.; Tsuboyama, S.; Nishio, M. *J. Chem. Soc., Perkin Trans 2* **2001**, 2053. (b) Nishio, M. *CrystEngComm* **2004**, *6*, 130. (c) Re, S.; Nagase, S. *Chem. Commun*. **2004**, 658. (d) Desiraju, G. R.; Steiner, T. *The Weak Hydrogen Bond in Structural Chemistry and Biology*; Oxford University Press: Oxford, U.K., 1999. (e) Steiner, T. *Angew. Chem., Int. Ed*. **2002**, *41*, 48.

(4) (a) Ferguson, G.; Glidewell, C.; Lough, A. J.; McManus, G. D.; Meehan, P. R. *J. Mater. Chem*. **1998**, *8*, 2339. (b) MacGillivray, L. R.; Reid, J. L.; Ripmeester, J. A. *CrystEngComm* **1999**, *1*, 1. (c) Scott, J.; Asami, M.; Tanaka, K. *New J. Chem*. **2002**, *26*, 1822. (d) Hoger, S.; Morrison, D. L.; Enkelman, V. *J. Am. Chem. Soc*. **2002**, *124*, 6734. (e) Caira, M. R.; Horne, A.; Nassimbeni, L. R.; Toda, F. *J. Mater. Chem*. **1997**, *7*, 2145. (f) Ma, B.-Q.; Zhang, Y.; Coppens, P. *Cryst. Growth Des*. **2002**, *2*, 7. (g) Huang, K.-S.; Britton, D.; Etter, M. C.; Byrn, S. R. *J. Mater. Chem*. **1997**, *7*, 713.

(5) MacGillivray, L. R. *CrystEngComm* **2002**, *4*, 37.

(6) (a) Ermer, O.; Eling, A. *J. Chem. Soc., Perkin Trans 2* **1994**, 925. (b) Corradi, E.; Meille, S. V.; Messina, M. T.; Metrangolo, P.; Resnati, G. *Angew. Chem., Int. Ed.* **2000**, *39*, 1782. (c) Papaefstathiou, G. S.; MacGillivray, L. R. *Org. Lett*. **2001**, *3*, 3835. (d) MacGillivray, L. R.; Reid, J. L.; Ripmeester, J. A. *J. Am. Chem. Soc*. **2000**, *122*, 7817. (e) Biradha, K.; Zaworotko, M. J. *J. Am. Chem. Soc*. **1998**, *120*, 6431. (f) Aitipamula, S.; Nangia, A.; Thaimattam, R.; Jaskólski, M. *Acta Crystallogr., Sect. C: Cryst. Struct. Commun*. **2003**, *59*, 481. (g) Vangala, V. R.; Bhogala, B. R.; Dey, A.; Desiraju, G. R.; Border, C. K.; Smith, P. S.; Mondal, R.; Howard, J. A. K.; Wilson, C. C. *J. Am. Chem. Soc*. **2003**, *125*, 14495.

(7) (a) Lavender, E. S.; Glidewell, C. *Acta Crystallogr., Sect. C: Cryst. Struct. Commun*. **1999**, *55*, 1489. (b) Ma, B.-Q.; Coppens, P. *Chem. Commun*. **2003**, 504. (c) Tanaka, T.; Tasaki, T.; Aoyama, Y. *J. Am. Chem. Soc*. **2002**, *124*, 12453. (d) MacGillivray, L. R.; Reid, J. L.; Ripmeester, J. A. *CrystEngComm* **1999**, *1*, 1. (e) Aitipamula, S.; Desiraju, G. R.; Jaskólski, M.; Nangia, A.; Thaimattam, R. *CrystEngComm* **2003**, *5*, 447. (f) Vishweshwar, P.; Nangia, A.; Lynch, V. M. *CrystEngComm* **2003**, *5*, 164. (g) Gao, X.; Friscic, T.; MacGillivray, L. R. *Angew. Chem., Int. Ed*. **2004**, *43*, 232. (h) Zeng, Q.; Wu, D.; Liu, C.; Ma, H.; Lu, J.; Xu, S.; Li, Y.; Wang, C.; Bai, C. *Cryst. Growth Des*. **2005**, *5*, 1041 (i) Biradha, K.; Mahata, G. *Cryst. Growth Des*. **2005**, *5*, 61.

(8) (a) Ferguson, G.; Bell, W.; Coupar, P. I.; Glidewell, C. *Acta Crysallogr., Sect. B: Struct. Sci*. **1997**, *53*, 534. (b) Ferguson, G.; Coupar, P. I.; Glidewell, C. *Acta Crystallogr., Sect. B: Struct. Sci*. **1997**, *53*, 513. (c) Coupar, P. I.; Ferguson, G.; Glidewell, C. *Acta Crystallogr., Sect. C: Cryst. Struct. Commun*. **1996**, *52*, 2524. (d) Coupar, P. I.; Ferguson, G.; Glidewell, C. *Acta Crystallogr., Sect. C: Cryst. Struct. Commun*. **1996**, *52*, 3052.

(9) Moberg, C. *Angew. Chem., Int. Ed*. **1998**, *37*, 248.

(10) (a) Balasubramaniam, V.; Ling Guan, W.; Vittal, J. J.; Valiyaveettil, S. *Cryst. Growth Des*. **2004**, *4*, 553. (b) Jayaraman, A.; Balasubramaniam, V.; Valiyaveettil, S. *Cryst. Growth Des*. **2005**, *5*, 1575.

(11) Kelderman, K.; Starmans, W. A. J.; van Duynhoven, J. P. M.; Verboom, W.; Engbersen, J. F. J.; Reinhoudt, D. N. *Chem. Mater*. **1994**, *6*, 412.

(12) *SMART and SAINT Software Reference Manuals*, Version 6.22; Bruker AXS Analytical X-ray Systems, Inc.: Madison, WI, 2000.

(13) Sheldrick, G. M. *SADABS, Software for Empirical Absorption Correction*; University of Göttingen: Germany, 2000.

(14) *SHELXTL Reference Manual*, Version 5.1; Bruker AXS, Analytical X-ray Systems, Inc.: Madison, WI, 1997.

(15) (a) Ahn, P. D.; Bishop, R.; Craig, D. C.; Scudder, M. L. *Struct. Chem*. **1999**, *10*, 3. (b) Ung, A. T.; Bishop, R.; Craig, D. C.; Dance, I. G.; Scudder, M. L. *J. Chem. Soc., Perkin Trans. 2* **1992**, 861. (c) Kim, S.; Bishop, R.; Craig, D. C.; Dance, I. G.; Scudder, M. L. *J. Org. Chem*. **2002**, *67*, 3221.

(16) (a) McGaughey, G. B.; Gagné, M.; Rappe, A. K. *J. Biol. Chem*. **1998**, *273*, 15458. (b) Narasimhamurthy, T.; Benny, J. C. N.; Pandiarajan, K.; Rathore, R. S. *Acta Crystallogr., Sect. C: Cryst. Struct. Commun*. **2003**, *59*, 620. (c) García-Báez, E. V.; Martínez-Martinez, F. J.; Höpfl, H.; Padilla-Martínez, I. I. *Cryst. Growth Des*. **2003**, *3*, 35.

(17) (a) Balasubramaniam, V.; Saifudin, M. A.; Vittal, J. J.; Valiyaveettil, S. *CrystEngComm* **2004**, *6*, 284. (b) Thalladi, V. R.; Smolka, T.; Gehrke, A.; Boese, R.; Sustmann, R. *New J. Chem*. **2000**, *24*, 143.

CG050251P